Numerical simulations of fatigue crack initiation and propagation based on re-tensile plastic zone generating load criterion for in-plane gusset welded joints

Nagata, Yukinobu
Department of Civil and Structural Engineering, Graduate School of Engineering, Kyushu University

Gotoh, Koji
Department of Marine Systems Engineering, Faculty of Engineering, Kyushu University

Toyosada, Masahiro
Kyushu University: Professor Emeritus

出版情報：Journal of Marine Science and Technology. 14, pp.104-114, 2009-02-18. Japan Society of Naval Architects and Ocean Engineers (JASNAOE)
バージョン：
権利関係：

Abstract

Welded built-up steel structures in service encounter many accidents caused by fatigue, and it is important for maintenance of social foundations and safeness to estimate their fatigue lives quantitatively.

By considering that fatigue cracks cannot grow without the accumulation of alternating tensile / compressional plastic strain, one of the authors identified that the improved effective stress intensity factor range ΔK_{RPG} based on the Re-tensile Plastic zone Generating (RPG) load which represents the fatigue crack driving forces, and suggested that ΔK_{RPG} should be applied as the parameter in order to describe the fatigue crack growth behavior. For predicting fatigue crack initiation and propagation behavior, numerical simulation code "FLARP", which ΔK_{RPG} is implemented as the fatigue crack growth parameter was developed.

In this paper, it is confirmed that fatigue life estimation by FLARP gives accurate results by comparing the estimated fatigue crack growth curves and $S-N$ curves with the experimental results for in-plane gusset welded joints, which are used in many welded steel structures. Moreover, the effect of induced bending moment due to the linear misalignment for out of plane direction on the fatigue strength of in-plane gusset welded joints is investigated by the numerical simulations.

Key words

Fatigue, Re-tensile Plastic zone Generating (RPG) load, Numerical Simulations of Fatigue Crack Initiation and Propagation, FLARP, In-plane Gusset Welded Joints

TEXT

1 Introduction

Although the fatigue crack growth curve should be given for constructions of anti-fatigue damage and for repair plans of fatigue damages, fatigue crack growth behavior does not considered in the conventional fatigue design for welded built-up steel structures, because the conventional fatigue design for the structures are performed by applying the combination of $S-N$ curves in many design codes and cumulative damages law, i.e. Miner's rule. In addition, it is not clear the transferability of fatigue life between specimens and in-service large structures[1].

On the other hand, fatigue crack growth curves are estimated by applying conventional fatigue crack propagation laws, e.g. Paris' law or Elber's law, if required. However, conventional propagation laws cannot evaluate the various transient phenomena quantitatively, e.g. retardation and acceleration of crack propagation, because of insufficient consideration of fatigue crack opening / closing behavior caused by crack wake. Therefore, improved fatigue crack growth law is required in order to estimate the fatigue crack growth curves quantitatively.

Many fatigue damages in steel structures are often found in stress concentration fields, and fatigue cracks initiate from stress concentration fields even though no initial defect exists in the region. Hence, it is required for quantitative assessments of fatigue life in order to estimate the continuous fatigue crack growth curves from initial defect-free sites in stress concentration fields.

By considering that fatigue cracks cannot grow without the accumulation of alternating tensile / compressional plastic strain, one of authors identified that the effective stress intensity factor range ΔK_{RPG} based on the re-tensile Plastic Zone Generation (RPG) load which represents the fatigue crack driving force. ΔK_{RPG} is formulated by replacing the crack opening load with RPG load. The authors suggest that ΔK_{RPG} should be applied as the fatigue parameter in order to describe the fatigue crack growth behavior[2,3]. Besides, in order to estimate continuous fatigue crack growth curves initiating from stress concentration fields, the equivalent ΔK_{RPG} in the first stage of fatigue crack growth which corresponds to the fatigue crack initiation and propagation to the first grain boundary is defined by considering the dislocation behaviors in the vicinity of a crack initiation region[4].

Numerical simulation code FLARP, which implemented ΔK_{RPG} criterion for fatigue crack growth law, is proposed by authors[4]. The validity of proposed method is confirmed by comparing with measured fatigue crack growth curve of boxing fillet weld joint with stiffener[4].

In this paper, the validity of fatigue life estimation by FLARP for in-plane gusset welded joints is investigated by comparing with the experimental results, fatigue crack growth curves and $S-N$ curves. Although in-plane gusset welded joints are very popular and used in many welded structures, few researches are reported for their fatigue performance including crack growth curves.

2 Features of fatigue life estimation by FLARP

Features of fatigue life estimation code FLARP are summarized as fellows.

2.1 Continuous analysis of fatigue crack initiation and propagation

In the early stage of fatigue damages occurred in stress concentration sites, slip bands generate near material surface, e.g. notch root. These slip bands grow to shear mode crack, and finally grow to opening mode crack[5]. Shear mode crack generated near material surface grows without showing crack opening / closing behavior until crack reaches at the first grain boundary. Next, crack starts to opening / closing behavior following by crack propagation. Stress distribution over a crack line keeps constant during the crack propagation in the first grain because shear mode crack does not show the crack opening / closing behavior.

By considering that fatigue crack cannot propagate without alternating tensile / compressional plastic behavior ahead of a crack tip and that stress redistribution does not occur during shear mode crack, RPG load during shear mode crack propagates in the first grain and the equivalent ΔK_{RPG} can be formulated[4]. Hence, it is possible that fatigue crack growth curves are estimated without setting initial crack, which means the continuous calculation of fatigue crack initiation and propagation methodology is established.

2.2 Evaluation of multiple surface cracks growth and coalescence behavior

Generally, fatigue cracks occurred in stress concentration regions are multiple surface cracks. These surface cracks coalesces and then to form one large surface crack. These processes are very complex and it is impossible to perform numerical simulations of multiple surface cracks growth directly at present. Therefore, authors proposed the representative single surface crack which enables to generate the same stress-strain field of multiple surface cracked fields. Besides, the estimation procedure of the aspect ratio of a representative surface crack from the stress distribution of the same bodies without cracks is proposed[4]. A representative surface crack has equal crack depth of the deepest surface crack existed in the reference region.

By using above concept, the growth and coalescence processes of multiple surface cracks can be treated as the ones of a representative single surface crack.

2.3 Equivalent distributed stress

The shape of fatigue crack is not through thickness crack but surface crack in the early stage of crack growth. It is very complicated to perform the quantitative numerical simulation of surface crack opening / closing behaviors which affects crack propagation.

For above reason, Equivalent Distributed Stress (EDS) is proposed[4]. EDS corresponds to the stress distribution of a through thickness crack in an infinitely wide plate and gives the same stress

intensity factor histories of the objects according to crack extension. FLARP adopted EDS in order to avoid the surface crack growth simulation directly.

3 Fatigue life assessment flow by FLARP

Fatigue life estimation procedure by FLARP is shown Fig.1 and summarized below.

1. Calculation of the stress distributions around fatigue crack growth region under the unit external stress amplitude, dead load (mean stress) and pre-existing residual stress field by numerical analyses, e.g. FEM.
2. Identification of the fatigue crack propagation path. Fatigue crack propagates normal to direction of the applied maximum principal stress[6,7].
3. Calculation of the normal component of stresses along assumed crack path.
4. Estimation of the change of aspect ratio of a representative fatigue surface crack. The shape of representative fatigue surface crack can be approximated to an ellipse until full penetration of the wall thickness. The changing manner of the representative aspect ratio of surface cracks near a fillet weld toe in the as-welded condition is also proposed by authors[4].
5. Calculation of the stress intensity factors under each stress distribution. In these calculations, the girth length of assumed crack path replaces the straight line for the convenience. The stress intensity factors for a surface crack under arbitrary stress fields can be approximated by using

the improved superposition method[4] based on the method proposed by Maddox[8].

6. Transformation of the each stress distribution into the Equivalent Distributed Stresses.

7. Fatigue crack growth simulation by FLARP.

4 Fatigue test

Specimen configurations of in-plane gusset welded joints are shown in Fig.2. Gusset joints are connected to the main plate by using CO_2 arc welding. Single bevel grooves are cut on front surface of weld locations. Fabrication order is 1) two passes welding on front side, 2) gouging of root, 3) two passes welding on back surface. Welding conditions are shown in Table1.

The cases of nominal stress ranges shown in Table2 are applied. Cyclic frequencies of all tests are 10Hz. Material used is SM490Y steel of Japan Industrial standards and yield stress of the material is equal to 398MPa. Measurements of crack length are performed by the beach mark method (five points average method). An example of loading histories is shown in Fig.3.

Although yield stress under cyclic loading are necessary in order to simulate the fatigue crack growth in the first grain by FLARP, no date are obtained for applied material. Then, yield stress under cyclic loading of the material is estimated by multiplying yield stress under static loading obtained from mil sheet by 0.545, which value is for mild steel and is measured by authors[4].

5 Estimation of crack initiation and propagation life of in-plan gusset welded joints

5.1 Stress distribution under external unit loading

Stress distribution under external unit loading is calculated by elastic FE analysis. The commercial finite element analysis code MSC Nastran 2004r2 is applied. FEM model is shown in Fig.4. Analyses are performed with upper half of the specimen, because fatigue crack initiates from one side of weld toe of gusset joints and propagates through whole main plate. The specimen is modeled using three-node and four-node isoparametric elements. Number of nodes and elements are respectively 21587 and 21428 respectively. The minimum element size is 0.5×0.5 mm. The material is SM490Y steel of Japanese Industrial Standards.

5.2 Estimation of welding residual stress

Most of fatigue cracks in the steel welded built-up structures initiate from weld toe. Peak value of residual stresses in the crack initiation region reaches yield stress in case that the steels which tensile strength is below 500 MPa are applied.

It is considered that tensile residual stress reduces fatigue life. On the other hand, the compressive residual stress raises fatigue life because crack propagation rate decreases in the compressive residual stress region. Hence, it is necessary to calculate precise residual stress distributions in order

to estimate fatigue life quantitatively.

Residual stress distributions are analyzed by elastic FE analysis in consideration of the inherent stress method[9]. The inherent stress corresponds to the source of residual stresses, and it can be expressed as a function of heat input by welding and yield stress of materials. In the case of in-plane gusset welded joints, the inherent stress is given in regions (I), (II) and (III) shown in Fig.5, because main plate and gusset plates are connected by butt weld and boxing weld for dressing of both end of butt weld.

In the region (I), (II) and (III), the inherent stress σ^{Ia} generated by butt weld of main plate and gusset joint can be calculated by applying the following general formulation of the inherent stress distribution[10].

$$
\begin{aligned}
&\sigma^{Ia}(x,y,z) = \int_0^L g\big(X(t)-x, Y(t)-y\big)dt, \\
&g(x,y,z) = \alpha\sigma_Y \exp\big(-\pi(x^2+y^2)/B^2\big) f(z:T)/B, \\
&f(z:T) = \sum_{n=0}^{\infty} \exp\big(-\pi(\lambda z_n/B)^2\big), \\
&z_n = \big|z + \{(-1)^n(n+0.5) - 0.5\}T\big|, \\
&B = \beta\sqrt{\gamma Q/\sigma_Y},
\end{aligned}
\tag{1}
$$

where, $\alpha = 1.942$, $\beta = 1.357$, $\gamma = 0.16$, $\lambda = 1.788$, L: weld length, t: parameter to identify the location on weld line $(0 \le t \le L)$, $X(t), Y(t)$: coordinates on the weld line, Q: nominal heat input given by weld condition and T: plate thickness.

The inherent stress σ^{Ib} generated by boxing welding can be calculated by applying Equation (2)[11], which corresponds to the general formulation of inherent stress for fillet weld[10:]

$$\sigma^{Ib}(x,y,z) = \alpha\sigma_Y \exp\left(-\pi(x'/B)^2\right) f(|y'|:T), \tag{2}$$

where, $\lambda = 2.195$, (x', y') : coordinates which its origin is shown as O' in Fig.5.

The inherent stress σ^I in the region (I), (II) and (III) shown in Fig.5 can be obtained as the maximum value of inherent stresses given by each weldings[11].

$$\sigma^I = \max(\sigma^{Ia} + \sigma^{Ia'}, \sigma^{Ib}),$$

where, $\sigma^{Ia'}$ corresponds to the additional inherent stress[11] caused by the mirror effect due to free edges. The mirror effect concept is illustrated in Fig.6.

σ^I is inputted as the source of residual stresses. Calculations are performed by the finite element code MSC Nastran 2004r2. FEM model for residual stress calculation is the same with Fig.4.

Fig.7 is comparison of calculated residual stress distributions with measured ones. Measured locations of stresses are shown in Fig.2.

Because calculated stresses are good agreement with measured ones, it is confirmed that residual stress distribution in in-plane gusset welded joints can be estimated by the method used in this study.

5.3 Fatigue crack path and stress distribution along crack path

Crack propagation path is set under the assumption that crack propagates normal to the direction

of maximum principal stress under the external loading[6]. Estimated crack propagation path for the specimens is shown in Fig.8. It is confirmed that the tendency of estimated crack path is similar to experimental results by the observation of specimen.

Stress distributions along the crack path are shown in Fig.9. Solid curve and circle mark represent stress distribution under external unit loading. Detailed stress distribution near weld toe is estimated by using the formula[12] for the stress distribution near a notch root. Average radius of measured weld toe 1.5mm is applied to estimate stress distribution near weld toe. Dashed curve and triangle mark shown in Fig.9 represent residual stress distribution along the crack path.

5.4 Setting of the aspect ratio of a representative surface crack

As described in subsection 2.2, it is impossible to perform the direct numerical simulation of the growth of multiple surface cracks generated from many parts. Therefore, this growth process is replaced by introducing a representative single surface crack mentioned above, and the changing manner of aspect ratio of a representative surface crack following by a crack growth is proposed[4]. In this method, it is assumed that the shape of a representative surface crack which reaches first grain boundary is a half circle average grain size in diameter.

Supposed aspect ratio change of a representative surface crack is shown in Fig.10. The measured average grain diameter $30\,\mu$m is applied to calculate the aspect ratio change shown in Fig.10.

Discontinuous change of aspect ratio (crack depth $\simeq$ 0.4mm) corresponds to the point when one large surface crack develops through thickness crack.

5.5 Stress intensity factors

Stress intensity factors under the external unit loading and residual stress are calculated for crack extension along supposed crack path. These results are shown in Fig.11. Solid curves in this figure represent stress intensity factors for the external unit loading and dashed curves correspond to ones for the residual stresses.

Stress intensity factors for a representative surface crack under arbitrary stress field are calculated by the approximation superposition method[4]. Stress intensity factors for a through thickness crack are calculated by the integration of a single edge crack subjected to concentrated forces on the crack surfaces[13].

The region where stress intensity factors change drastically (crack depth $\simeq$ 0.4mm) corresponds to the transition region from the surface crack to the through thickness crack.

5.6 Equivalent distributed stress (EDS)

EDSs for external unit loading and residual stress are shown in Fig.12. Relationships between crack length and stress intensity factor shown in Fig.11 are used as input data for EDS distributions.

Solid curves in Fig.12 represent EDS under external unit loading and dashed curves correspond to EDS under residual stress fields.

6 Calculation results and discussion about in-plane gusset welded joints

6.1 Discussion about fatigue crack growth behavior

Comparison of estimated crack growth curves and experimental ones are shown in Fig.13. Two specimens are used in each load cases. Black and white circle marks in this figure represent experimental results of case1, while solid curve represents calculated one. Black and white triangle marks represent experimental results of case2, while dotted curve represents calculated one. Estimated crack growth curves by FLARP are in good agreement with the experimental ones. One experimental result plotted by white circle mark shows very good agreement with estimated one throughout total fatigue life.

However, other three experimental results show the difference from calculated ones at early stages of total fatigue life (crack length is less than 10mm). There is a possibility that these different crack growths are caused by different crack initiation and propagation process supposed in the numerical simulations. Observing the specimens, it is confirmed that weld joint has the linear misalignment for out of plane direction along weld line. Hence, it is presumed that out of plane bending was induced by this linear misalignment and quarter-elliptical corner crack initiated.

6.2 Fatigue crack growth behavior affected by the linear misalignment

Fatigue crack initiation and propagation simulations are performed under the condition that welded joint contains the linear misalignment. The width of misalignment which equals to 1mm is set as a representative value by the observation of specimens. The schematic illustration of supposed misalignment is shown in Fig.14. Stress distribution caused by external unit loading near weld toe under linear misalignment condition is shown in Fig.15. Stress distribution in this figure is dimensionless value normalized by maximum stress. Stress distribution changes not only along the crack depth direction (x axis in Fig.15)) but also the crack width direction (z axis in Fig.15) because of the existence of misalignment. The aspect ratio change of surface crack cannot be set under three dimensional stress distributions, because current estimated procedure of aspect ratio change cannot consider the effect of stress gradient to the surface crack width direction. Then, the aspect ratio change in the case of corner crack growth supposed as shown in Fig.16, because experimental crack growth behaviors show significant change at about 6mm of crack depth and the observation of crack surface after the experiments.

Stress distribution under external unit loading shown in Fig.15, and the aspect ratio change shown in Fig.16 are used as input data for calculation stress intensity factors and EDSs. These calculated results are shown in Fig.17 and Fig.18 respectively. Fatigue crack growth simulation considering the

linear misalignment effect is performed by FLARP with EDSs shown in Fig.18. Calculation results of crack growth curves are shown in Fig.19.

In Fig.19, fine solid and dashed curves correspond to estimated results without misalignment which are shown in Fig.13, while bold solid and dashed curves correspond to estimated results with misalignment.

On the results of case1, estimated total life is slightly different from experimental ones. However, the shape of estimated crack growth curve is similar to the experimental result (black circle) at early stage of measured total life. On the results of case2, estimated crack growth curves are in good agreement with experimental ones. Estimated crack growth curves considering misalignment show kink at 6mm of crack length, because the discontinuous jump of the stress intensity factor at 6mm of crack length (depth). This stress intensity factors jump is caused by the sudden change of crack shape from quarter-elliptical corner crack to through thickness crack, see Fig.16.

Estimated results without linear misalignment for case1 is in good agreement with experimental result represented as white circle mark throughout total fatigue life. Therefore, it is hypothesized that one specimen applied to the experiment case 1 has no linear misalignment. It is concluded that fatigue crack growth curves can be simulated by applying the algorithm proposed by the authors.

Estimated fatigue lives of the gusset specimens with misalignment are longer than them of normal specimens. The fatigue crack propagation ratio of a surface crack is lower than the ratio of a through

thickness crack in the circumstances which the depth of surface crack is equal to the length of through thickness crack and the same load range is applied to both two cracked bodies. The depth of a supposed corner crack is set about 6mm and the crack depth of normal specimen is about 0.4mm when crack shape changes to through thickness crack, see Figure 10. Therefore, specimens with misalignment keep longer period of surface crack shape during the total fatigue life than normal specimens.

7 Discussion about other experimental results

Kondo and Yamada[14] performed fatigue test in in-plane gusset welded joint specimens shown in Fig.20 under constant amplitude loading with frequency 10Hz and experimental results were reported as $S-N$ curves. The validity of fatigue life estimation algorithm developed by the authors is also investigated by comparing the estimated $S-N$ curves with the experimental results by Kondo and Yamada.

The applied minimum stresses for specimen GS and GL are equal to 10MPa. Gusset joints were connected to the main plate by using single groove (root gap is 2mm) using four weld passes (two passes each front and back surface of plate). The welding conditions for each specimen are shown in Table3. Material used is SM520B steel of Japanese Industrial Standards (JIS) and yield stress of the material is 402MPa. Although yield stress under cyclic loading is necessary for calculation of fatigue

life, no data are reported in the reference. Thus, a yield stress under cyclic loading for this material (SM520B) was estimated by applying the same method mentioned in section 4. The average grain diameter of material is set 30μm, according to subsection 5.4. Residual stress distributions are calculated by inherent stress method whose analysis procedure is described subsection 5.2.

Comparison estimated $S-N$ curves with experimental ones are shown in Fig.21. The crack initiation life and final failure life are plotted in these figures. The crack initiation life corresponds to the life until crack reaches the first grain boundary.

Although the estimated fatigue lives are longer than the experimental ones, estimated fatigue limits represented as mark of putting small black circle on large white circle and the slopes of estimated $S-N$ curves for each specimens are similar to those for the experimental results. Therefore, it is concluded that appropriate estimation of fatigue behavior is performed by FLARP although many unknown information including the definition of failure in these experiments exists under the numerical simulations.

8 Conclusions

Conventional fatigue strength evaluation methods based on $S-N$ curves are not enough for quantitative fatigue life predictions. The authors established the algorithm which enables simulation of the fatigue crack growth from the stress concentration field with zero defects and developed the

program code “FLARP” based on RPG load.

The validity of the fatigue life estimation by FLARP is confirmed by comparing estimated fatigue crack growth curves and $S-N$ curves with the experimental results for in-plane gusset welded joints. It is concluded that fatigue crack growth simulation code “FLARP” enables to estimate crack initiation and propagation behavior, i.e. total fatigue life without setting the initial crack length quantitatively.

In order to more accurate fatigue life evaluation, it is required that aspect ratio change of surface cracks under various stress fields is established. It is also considered that fatigue life evaluation adopting the effect of initial misalignment is performed if initial misalignment in welded built-up steel structures affects significantly fatigue crack behavior.

Acknowledgment

This research fund was Grant-in-Aid for Scientific Research (B)(2)(13450410) by Japan Society for the Promotion of Science.

References

1. Schütz W (1996) A HISTORY OF FATIGUE. Engineering Fracture Mechanics 54,2:263-300

2. Toyosada M, Niwa T (1994) The Significance of RPG load for fatigue crack propagation and the development of a compliance measuring system. International Journal of Fracture 67:217-230

3. Toyosada M, Gotoh K, Niwa T (2004) Fatigue crack propagation for a through thickness crack; a crack propagation law considering cyclic plasticity near the crack tip. International Journal of

Fatigue 26,9:pp983-992

4. Toyosada M, Gotoh K, Niwa T (2004) Fatigue life assessment for welded structure without initial defects; an algorithm for predicting fatigue crack growth from a sound site. International Journal of Fatigue 26,9:993-1002
5. Wood W A (1958) Recent observation on Fatigue Failure in Metals. ASTM STP-237, pp110-121
6. Ship Research Panel No.169 (1981) Final report of Ship Research Panel No.169 (in Japanese). The Shipbuilding Research Association of Japan
7. Erdogan F, Sih G C (1963) On the Crack Extension in Plates Under Plane loading and Transverse Shear. Journal of Basic Engineering, Transactions of the ASME, Series D, 86:519-527
8. Maddox S J (1972) An Analysis of Fatigue Cracks in Fillet Welded Joint. The Welding Institute, E/49/72
9. Matsuoka K (1983) An Analytical Method on Residual Stresses in Welded Built-up Shell Structures (in Japanese). Journal of the Society of Naval Architects of Japan 85:210-217
10. Matsuoka K, Yoshii T (1996) Weld Residual Stress in Corner Boxing Joints. NK TECK BULLETIN, pp1-10
11. Matsuoka K, Takahashi I, Yoshii T, et al (1991) Effects of Plate Thickness and Heat Input on Fatigue Strength of Non-Load-Carrying Fillet Welded Joints. IIW Doc. XIII-1407-91

12. Glinka G (1985) Calculation of Inelastic Notch-Tip Strain-Stress Histories under Cyclic Loading. Engineering Fracture Mechanics 22,5:839-864

13. Tada H, Paris P C, Irwin G R (2000) The Stress Analysis if Cracks Handbook (Third Edition), ASME International

14. Kondo A, Yamada K (2001) Fatigue tests by long-time variable amplitude loading (in Japanese). Fatigue Strength Research Committee in Japan Welding Society FS-1044-01

Tables

Table1 Welding conditions (CO_2 arc welding)

Current [A]	120
Voltage [V]	32
Travel speed [cm/min]	25.9

Table2 Loading conditions

	case 1	case 2
σ_{max} [MPa]	139	186
σ_{min} [MPa]	6	6
$\Delta\sigma$ [MPa]	133	183

Table3 Welding conditions and yield stress

Specimen type	GS	GL
Current [A]	110–120	160–175
Voltage [V]	25	25
Travel speed [cm/min]	9.5	14
Yield stress [MPa]	402	402

Figure legends

Fig.1 : Flow chart of fatigue crack growth simulation by FLARP

Fig.2 : Specimen configuration used

Fig.3 : An example applied loading history (case1)

Fig.4 : Finite element subdivision

Fig.5 : The region which different inherent stress distributions are applied

Fig.6 : The mirror effect concept of the inherent stress method

Fig.7 : Comparison of experimental and estimated residual stresses by FEM with the inherent stress method

Fig.8 : Supposed fatigue crack growth path on the specimen

Fig.9 : Stress distributions along the supposed crack path

Fig.10 : Supposed change of the aspect ratio of a representative surface crack

Fig.11 : Relationship between crack length and stress intensity factors

Fig.12 : Equivalent distributed stresses

Fig.13 : Comparison of experimental crack growth curves and calculated ones by FLARP

Fig.14 : The schematic illustration of linear misalignment

Fig.15 : Dimensionless stress distribution near the weld toe under misalignment condition

Fig.16 : Case of supposed change of the aspect ratio

Fig.17 : Relationship between crack length and stress intensity factors under supposed linear misalignment condition

Rig.18 : EDSs distribution under supposed linear misalignment condition

Fig.19 : Comparison of experimental crack growth curves and calculated ones under the assumption that a corner crack is generated by FLARP

Fig.20 : Specimen configurations by Kondo and Yamada

Fig.21 : Comparison of estimated $S-N$ curves by FLARP with experimental data

Figures

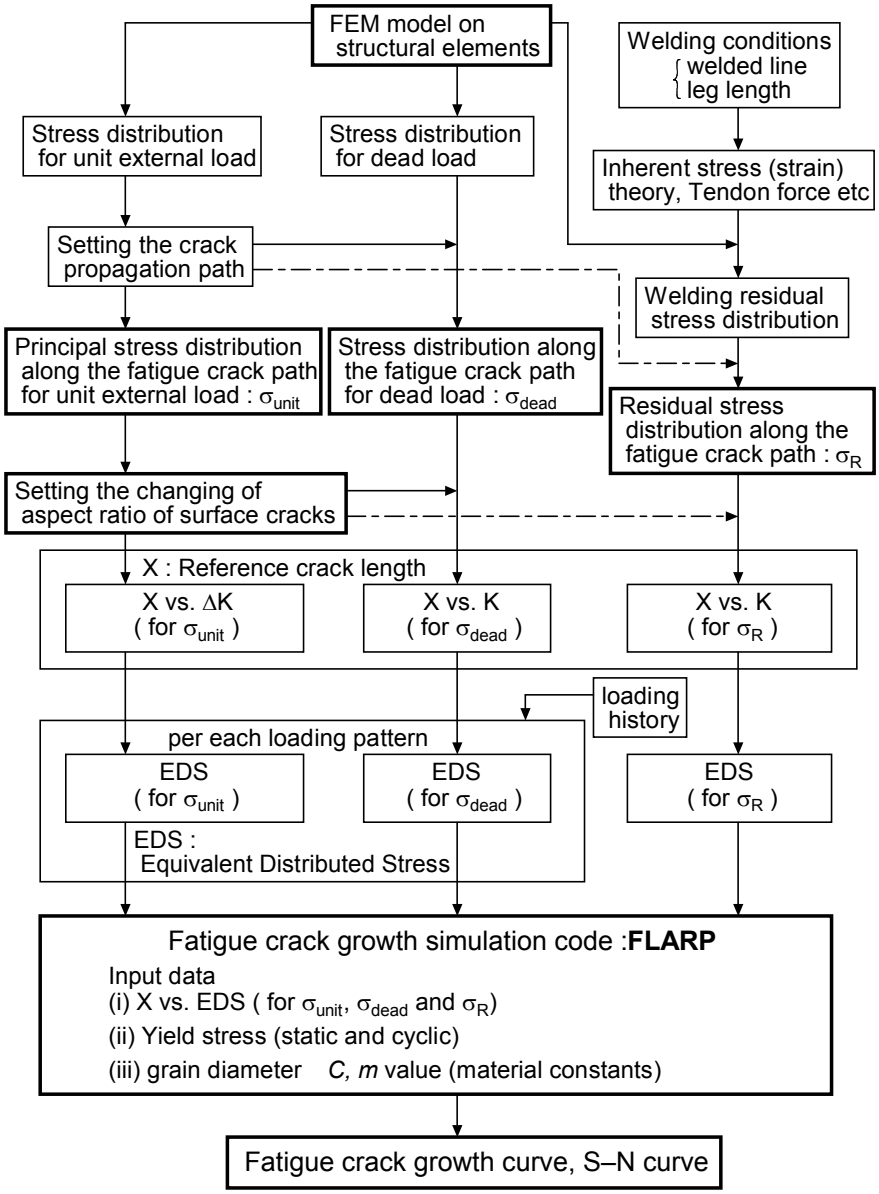

Fig.1

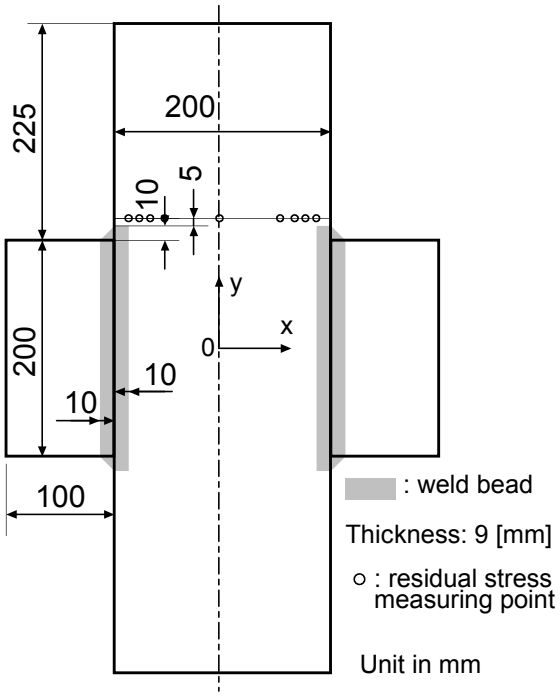
225
200
10
5
y
x
0
200
10
10
100
: weld bead
Thickness: 9 [mm]
○ : residual stress measuring point
Unit in mm

Fig.2

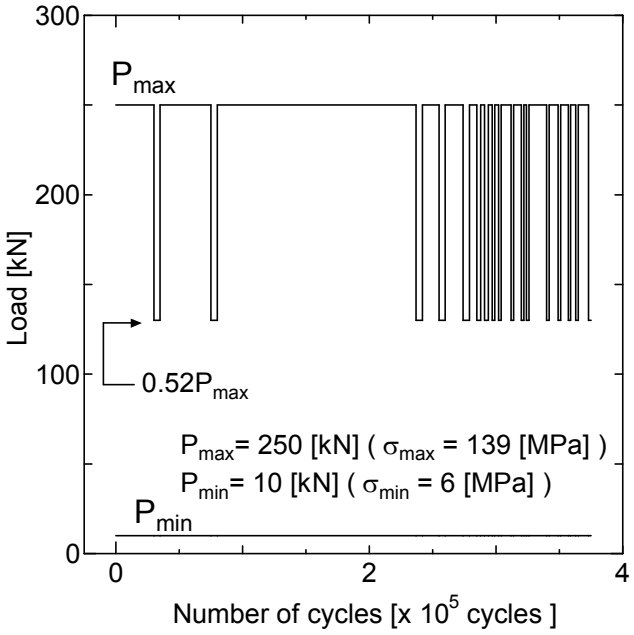
300
200
100
0
Load [kN]
P_{max}
$0.52P_{max}$
P_{max}= 250 [kN] (σ_{max} = 139 [MPa])
P_{min}= 10 [kN] (σ_{min} = 6 [MPa])
P_{min}
0
2
4
Number of cycles [x 10^5 cycles]

Fig.3

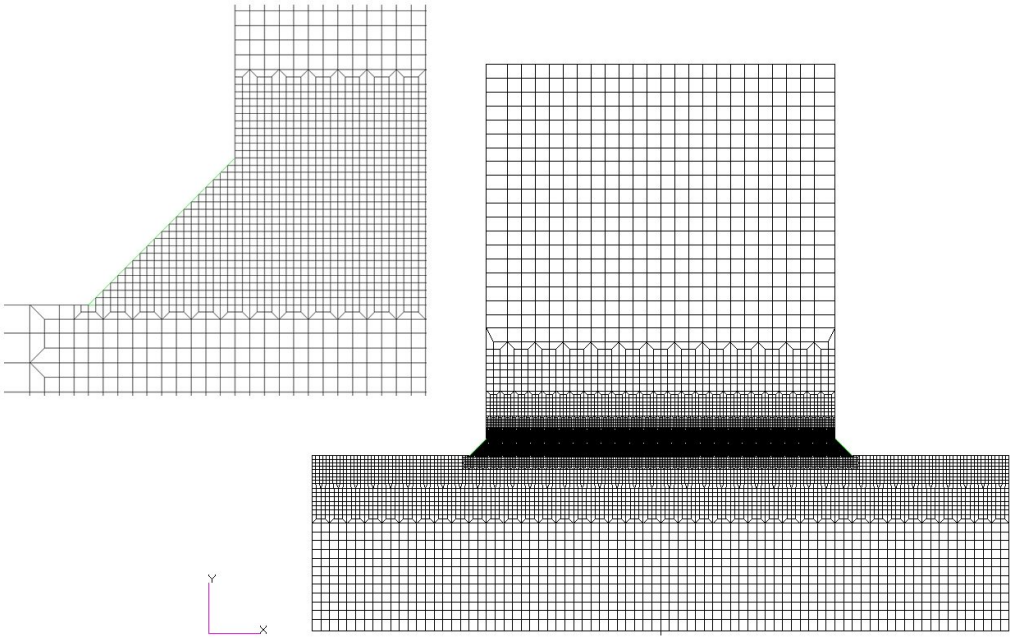

Fig.4

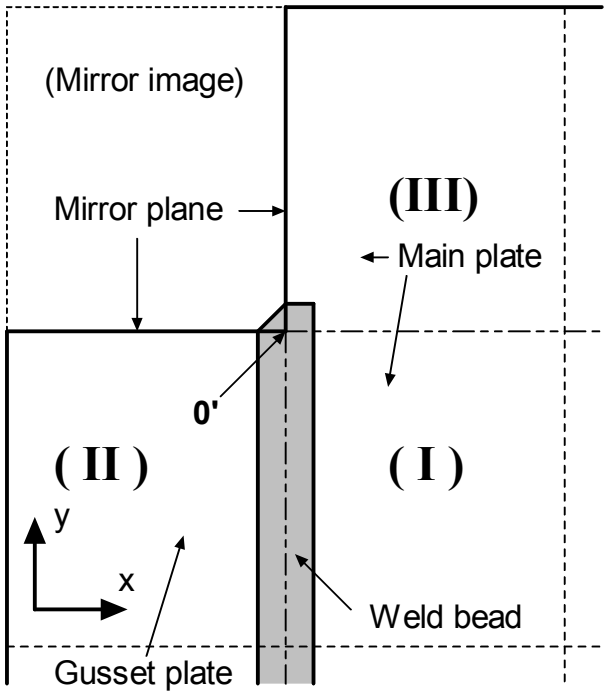
(Mirror image)
Mirror plane
(III)
Main plate
0'
(II)
(I)
y
x
Weld bead
Gusset plate

Fig.5

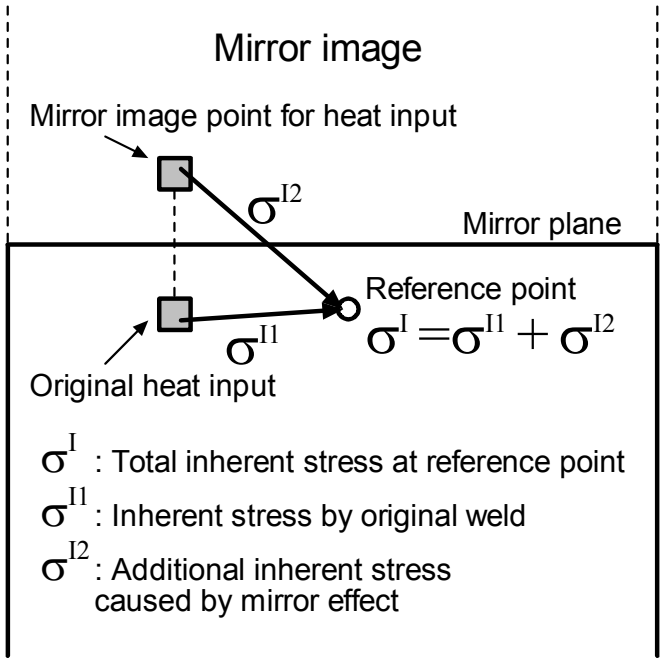
Mirror image
Mirror image point for heat input
σI2
Mirror plane
Reference point
σI = σI1 + σI2
σI1
Original heat input
σI : Total inherent stress at reference point
σI1 : Inherent stress by original weld
σI2 : Additional inherent stress
caused by mirror effect

Fig.6

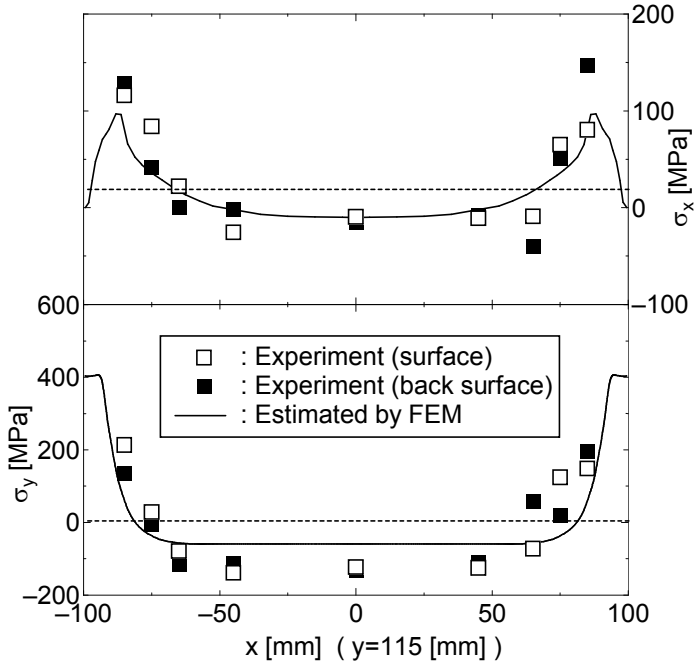
200
100
0
−100
σx [MPa]
600
400
200
0
−200
σy [MPa]
: Experiment (surface)
: Experiment (back surface)
: Estimated by FEM
−100
−50
0
50
100
x [mm] (y=115 [mm])

Fig.7

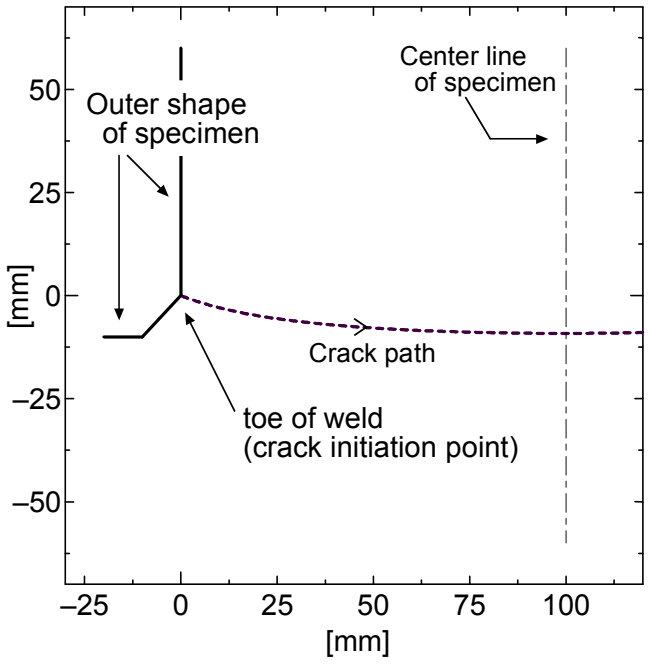
Center line
of specimen
Outer shape
of specimen
Crack path
toe of weld
(crack initiation point)
[mm]
[mm]
50
25
0
–25
–50
–25
0
25
50
75
100

Fig.8

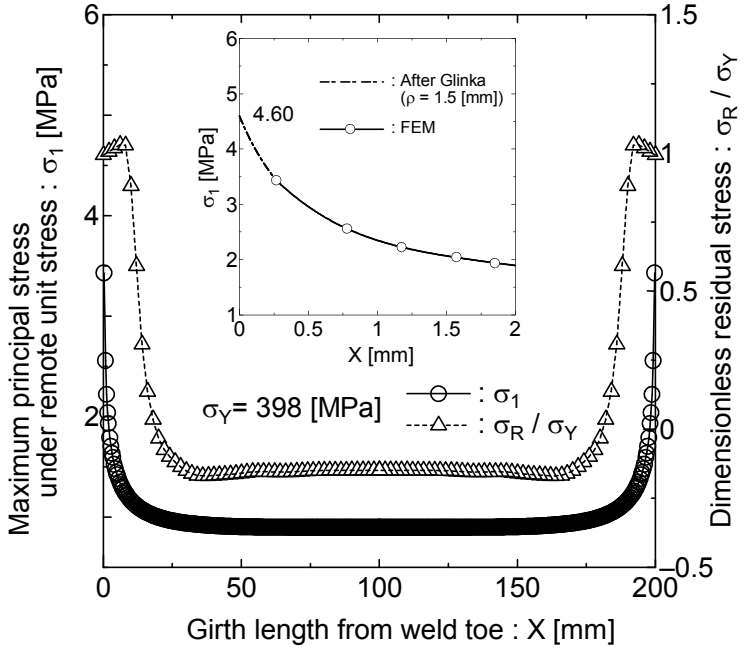
Maximum principal stress
under remote unit stress : σ1 [MPa]
Dimensionless residual stress : σR / σY
Girth length from weld toe : X [mm]
σY= 398 [MPa]
: σ1
: σR / σY
: After Glinka
(ρ = 1.5 [mm])
: FEM
4.60
σ1 [MPa]
X [mm]
0
50
100
150
200
2
4
6
–0.5
0
0.5
1
1.5

Fig.9

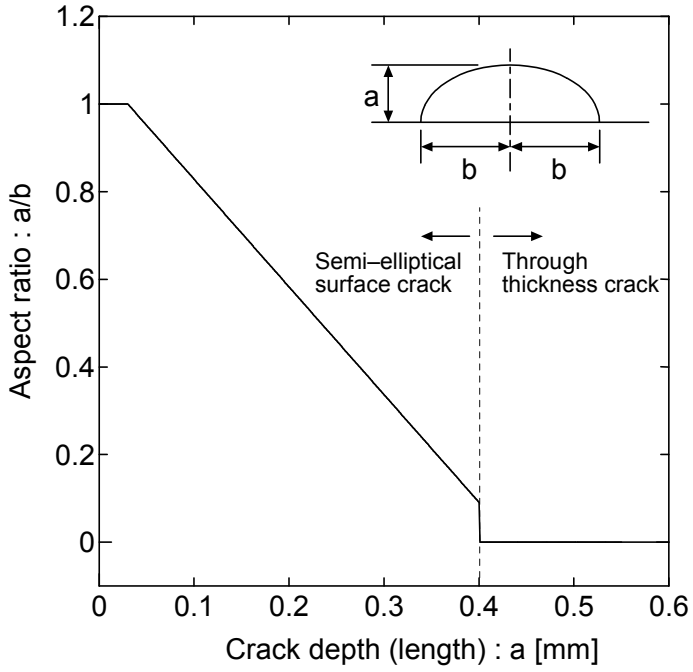
Aspect ratio : a/b
Crack depth (length) : a [mm]
a
b
b
Semi–elliptical surface crack
Through thickness crack

Fig.10

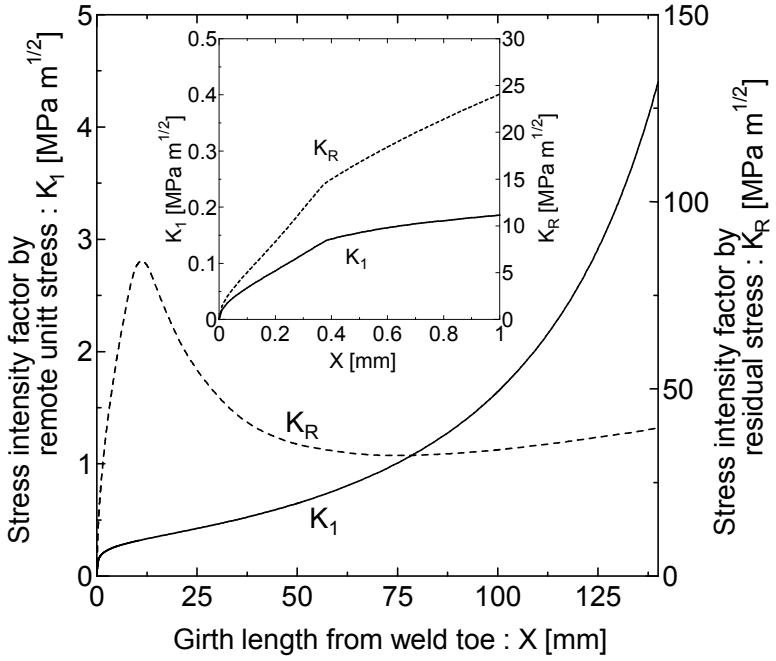
Stress intensity factor by remote unitt stress : K1 [MPa m1/2]
Stress intensity factor by residual stress : KR [MPa m1/2]
Girth length from weld toe : X [mm]
KR
K1
K1 [MPa m1/2]
KR [MPa m1/2]
X [mm]

Fig.11

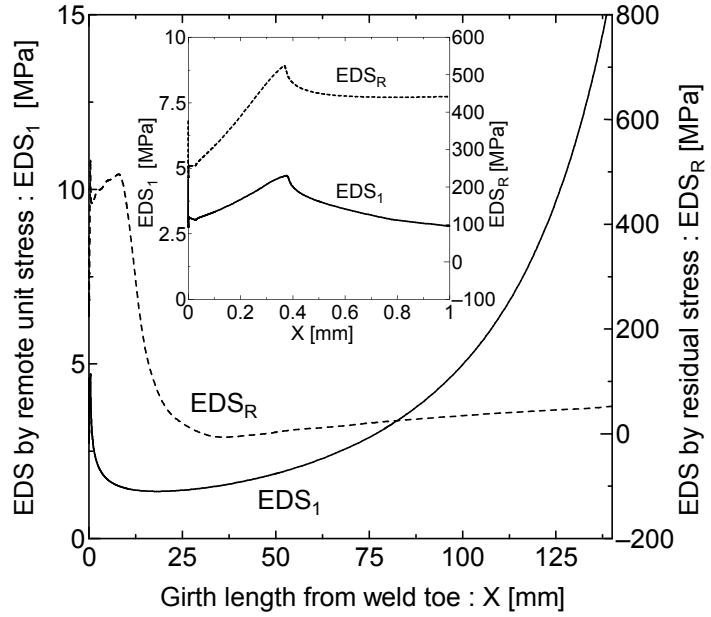
EDS by remote unit stress : EDS1 [MPa]
EDS by residual stress : EDSR [MPa]
Girth length from weld toe : X [mm]
EDSR
EDS1
EDS1 [MPa]
EDSR [MPa]
X [mm]

Fig.12

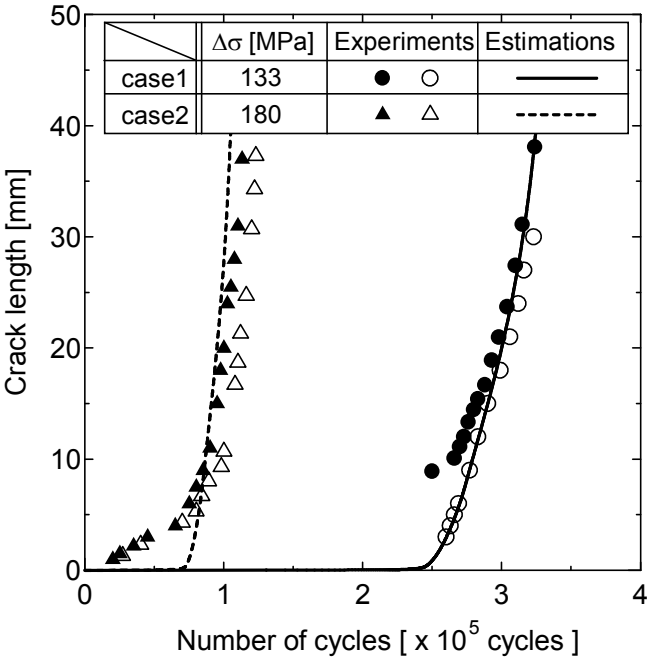
Δσ [MPa]
Experiments
Estimations
case1
133
case2
180
Crack length [mm]
Number of cycles [x 10^5 cycles]

Fig.13

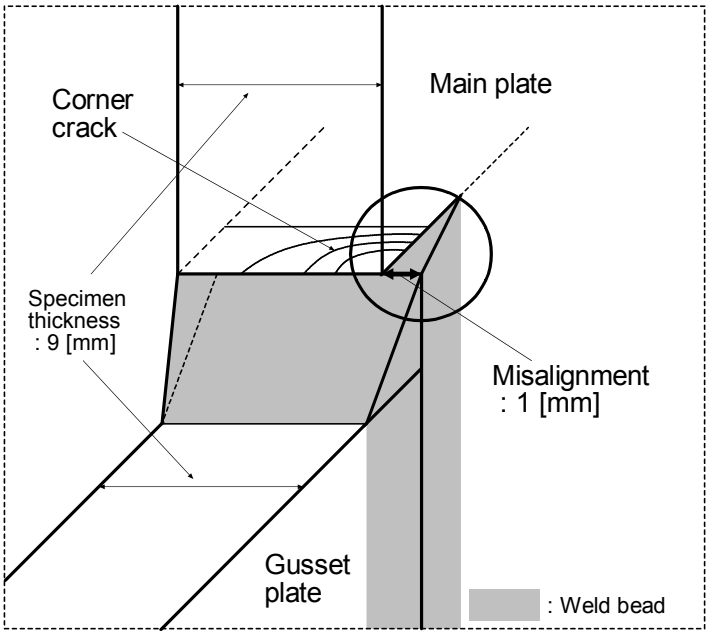
Corner
crack
Main plate
Specimen
thickness
: 9 [mm]
Misalignment
: 1 [mm]
Gusset
plate
: Weld bead

Fig.14

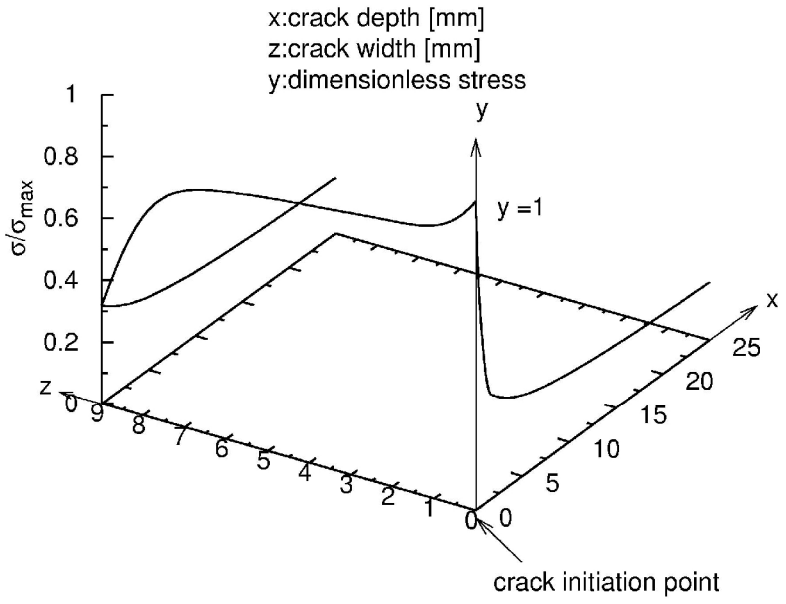
x:crack depth [mm]
z:crack width [mm]
y:dimensionless stress
y
y =1
σ/σmax
1
0.8
0.6
0.4
0.2
z
0
9
8
7
6
5
4
3
2
1
0
x
0
5
10
15
20
25
crack initiation point

Fig.15

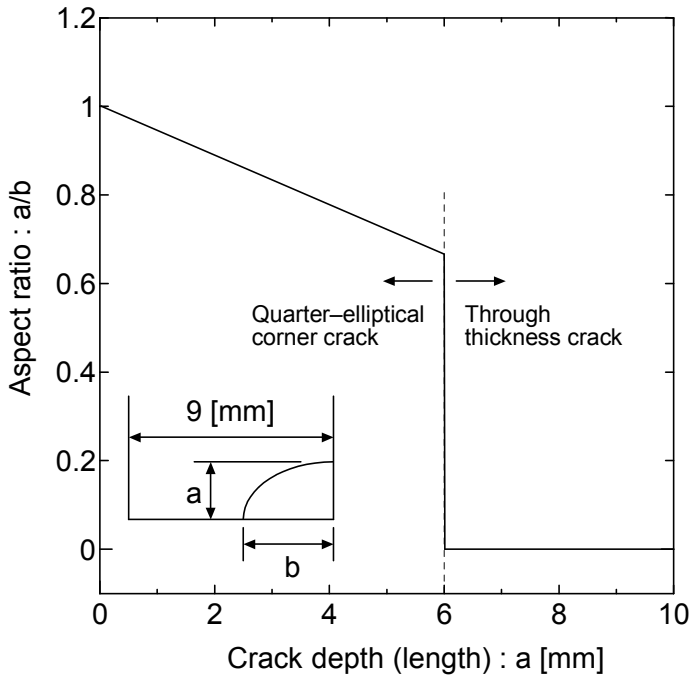
Aspect ratio : a/b
Crack depth (length) : a [mm]
Quarter–elliptical
corner crack
Through
thickness crack
9 [mm]
a
b

Fig.16

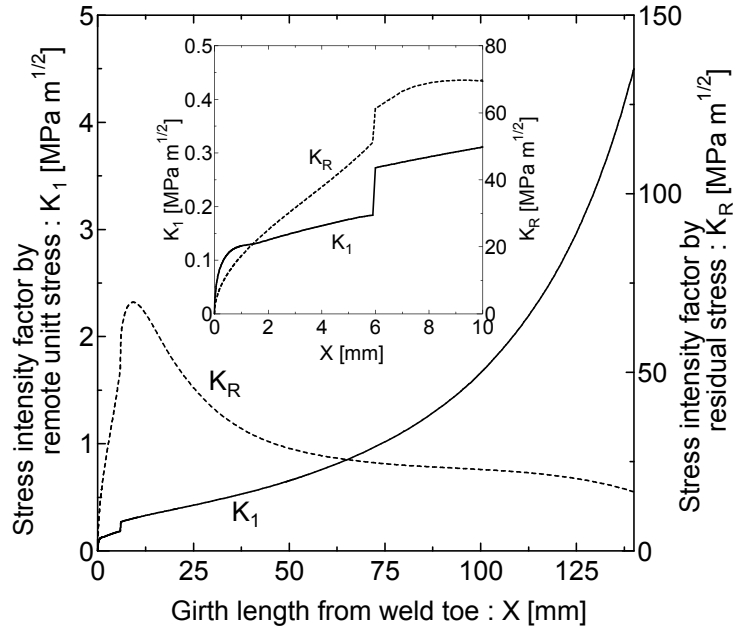
Stress intensity factor by
remote unitt stress : K1 [MPa m1/2]
Stress intensity factor by
residual stress : KR [MPa m1/2]
Girth length from weld toe : X [mm]
KR
K1
X [mm]

Fig.17

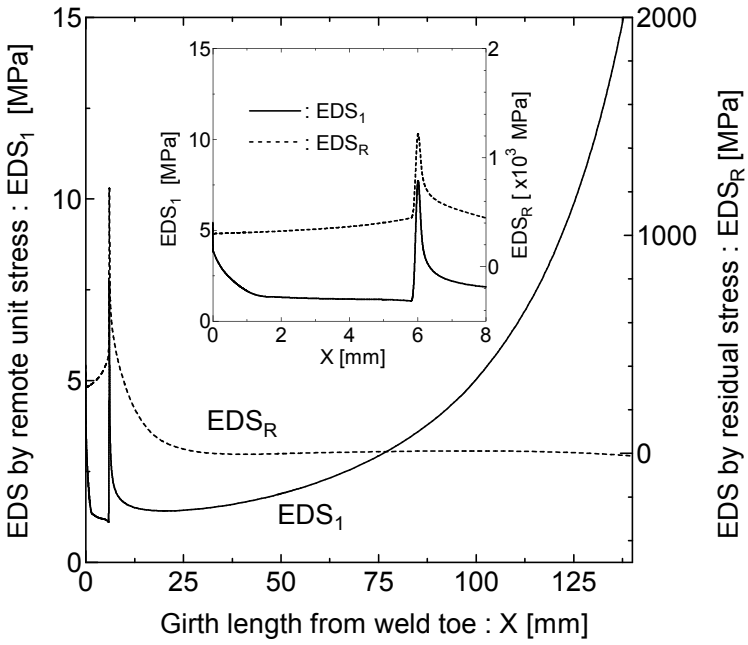
EDS by remote unit stress : EDS1 [MPa]
EDS by residual stress : EDSR [MPa]
Girth length from weld toe : X [mm]
EDSR
EDS1
: EDS1
: EDSR
EDS1 [MPa]
EDSR [x10^3 MPa]
X [mm]

Fig.18

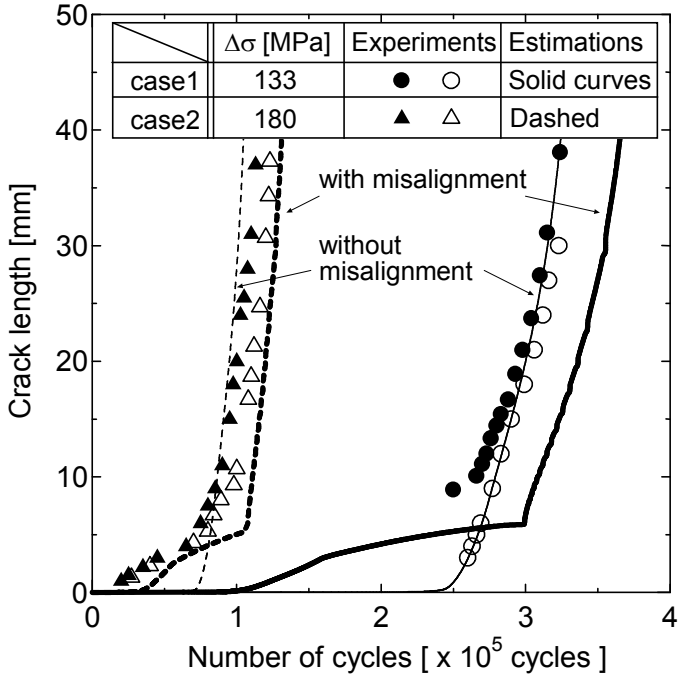
Δσ [MPa]
Experiments
Estimations
case1
133
Solid curves
case2
180
Dashed
with misalignment
without misalignment
Crack length [mm]
Number of cycles [x 10^5 cycles]

Fig.19

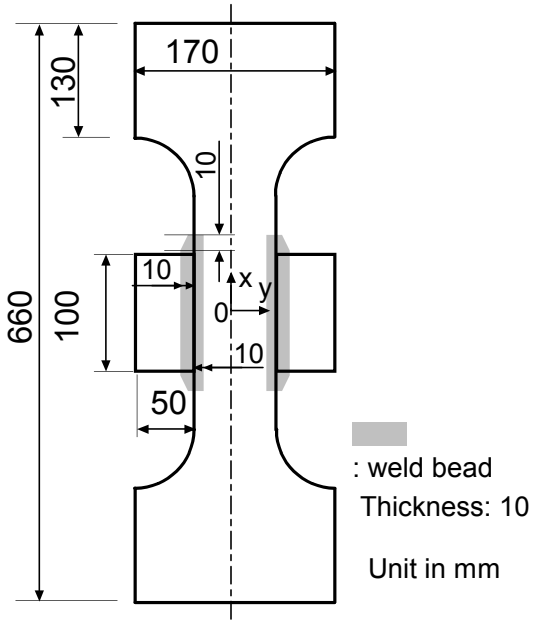

(a) Specimen GS

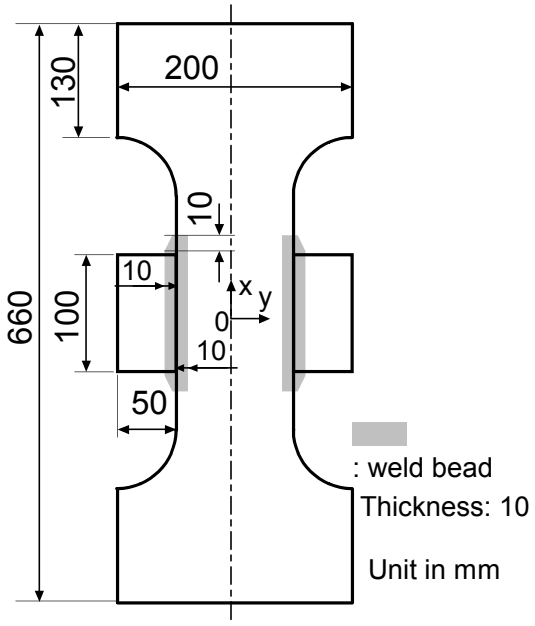

(b) Specimen GL

Fig.20

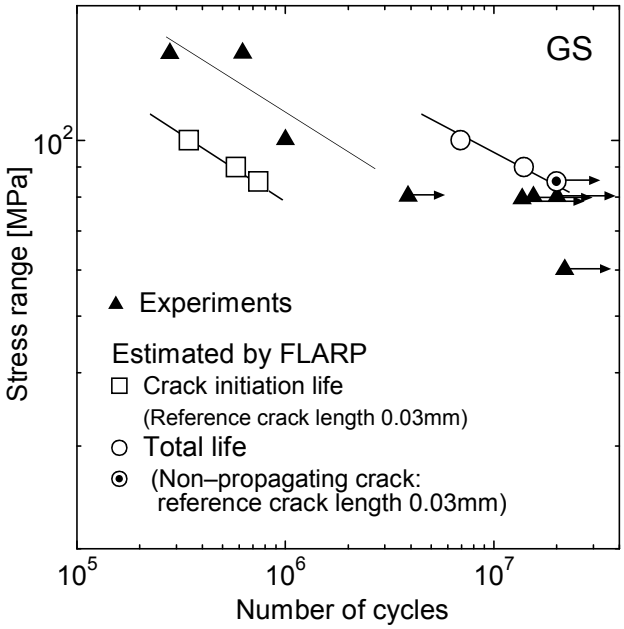

(a) Specimen GS

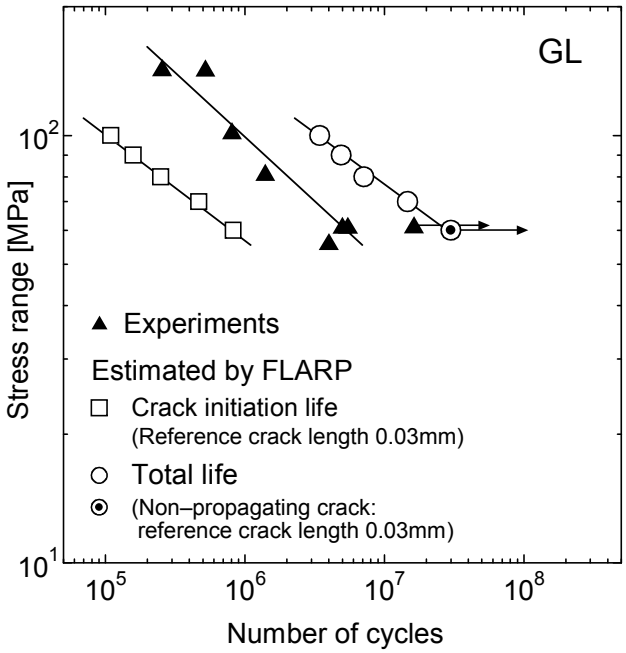

(b) Specimen GL

Fig.21